Submitted Manuscript

Title: Electrophysiological correlates of visual singleton detection

Authors: Daniel Tay, Victoria Harms, Steven A. Hillyard, John J. McDonald

DOI: 10.1111/psyp.13375

To appear in Psychophysiology

Please cite this article as: Tay, D., Harms, V., Hillyard, S. A., & McDonald, J. J. (in press). Electrophysiological correlates of visual singleton detection. *Psychophysiology*. https://doi.org/10.1111/psyp.13375

Electrophysiological Correlates of Visual Singleton Detection

Daniel Tay[1], Victoria Harms[1], Steven A. Hillyard[2], and John J. McDonald[1]

[1]Simon Fraser University

[2]University of California San Diego

Word Count (main text): 6,574

Author Note

Daniel Tay, Victoria Harms, and John J. McDonald, Department of Psychology, Simon Fraser University; Steven A. Hillyard, Department of Neurosciences, University of California San Diego. Victoria Harms is now at the College of Arts and Science, University of Saskatchewan.

This study was supported by the Natural Sciences and Research Council of Canada, Canadian Foundation for Innovation, and the Canada Research Chairs program.

D. T., V. H., S. A. H. and J. J. M. designed the experiment; D. T. and V. H. performed the experiment; D. T. and J. J. M. analyzed the data; D. T., S. A. H. and J. J. M. wrote the manuscript.

Correspondence and requests for materials should be addressed to Daniel Tay or John McDonald, Department of Psychology, Simon Fraser University, 8888 University Drive, Burnaby, B.C., Canada, V5A 1S6. E-mail: daniel_tay@sfu.ca (D. T.) or jmcd@sfu.ca (J. J. M.)

Abstract

Identifying a fixed-feature singleton that pops out from an otherwise uniform array of distractors elicits an event-related potential (ERP) component called the N2pc over the posterior scalp. The N2pc has been used to track attention with millisecond accuracy, inform theories of visual selection, and test for specific attention deficits in clinical populations, yet it is still unclear what neuro-cognitive process gives rise to the component. One hypothesis is that the N2pc reflects a spatial filtering process that suppresses irrelevant distractors. In support of this hypothesis, Luck and Hillyard (1994) showed that the N2pc is eliminated when the features of the target and distractors switch unpredictably across trials so that participants cannot prepare to filter out irrelevant items. The present study aimed to replicate Luck and Hillyard's singleton detection experiment, but with modifications to enhance the N2pc signal and to gain statistical power. We show that orientation singletons do, in fact, elicit the N2pc as well as an earlier-onsetting and longer-lasting singleton detection positivity (SDP) over the occipital scalp when the target and distractor orientations swap randomly across trials. We conclude that spatial filtering might not play a major role in the generation of the N2pc and that the selection processes required to search for fixed-feature targets (in feature-search mode) are also engaged in the detection of variable-feature singletons (in singleton-detection mode).

Key words: attention, visual search, singleton detection mode, event-related potentials, N2pc

Impact Statement

The N2pc component of the visual event-related potential has been interpreted in terms of a mental operation that filters out visual distractors, primarily because one study found the N2pc to be absent in a task that discourages distractor filtering. The present study calls into question this interpretation by showing that the original null result was likely due to a lack of statistical power. A singleton detection positivity (SDP) was observed over the posterior scalp commencing just prior to the N2pc. We conclude that the SDP reflects processes associated with singleton detection and that N2pc reflects attentional processing of the attended item.

1. Introduction

In the early 1990s, researchers began to investigate visual search by recording event-related potentials (ERPs) that were time-locked to search arrays. It was quickly discovered that when observers were required to detect a specific feature singleton that "popped out" from an otherwise uniform field of task-irrelevant items, ERP waveforms recorded over the posterior scalp became more negative at electrodes positioned contralateral to the singleton than at electrodes positioned ipsilateral to the singleton (Luck & Hillyard, 1994a, 1994b). This lateralized voltage difference was labelled the posterior contralateral N2 (N2pc) to denote its scalp distribution and timing (approximately 200–300 ms; in the time range of the N2 peak). Several lines of evidence linked the N2pc to the focusing of attention upon individual items, or groups of items, within multi-item visual displays (for a review, see Luck, 2012). On the weight of this evidence, the N2pc has become the gold-standard electrophysiological marker of attentional focusing in visual search tasks, enabling researchers to track the covert deployment of attention with millisecond precision (e.g., Eimer & Grubert, 2014; Hickey, McDonald, & Theeuwes, 2006; Woodman & Luck, 1999, 2003), inform theories of visual selection (e.g., Luck, Girelli, McDermott, & Ford, 1997; Theeuwes, 2010), and determine whether specific groups of individuals have an impaired ability to focus attention on task-relevant targets (e.g., Gaspar, Christie, Prime, Jolicoeur, & McDonald, 2016; Luck & Gold, 2008; Wang, Sun, Sun, Huang, Tao et al., 2014).

Since its initial discovery, researchers have sought to identify the specific neuro-cognitive process, or processes, that give rise to the N2pc. One prevalent hypothesis is that the N2pc reflects a spatial filtering process that reduces the responsivity of visual cortical neurons to task-irrelevant distractors that are within the vicinity of a target (or, in some cases, a nontarget that

captures attention), so that the presence of such distractors does not interfere with the identification of the target (Luck, 2012; Luck et al., 1997; Luck & Hillyard, 1994a). One manifestation of the hypothesized spatial filter is that of an inhibitory band that surrounds an "attended" object and acts to suppress information arising from nearby distractors (e.g., Luck & Gold, 2008, Figure 1C). From this perspective, the results of recent clinical studies would indicate that children with ADHD have an impaired ability to filter out distractors, as indexed by a reduced-amplitude N2pc relative to their typically developing counterparts (Wang et al., 2016), whereas individuals with schizophrenia do not (because their N2pc does not differ from that

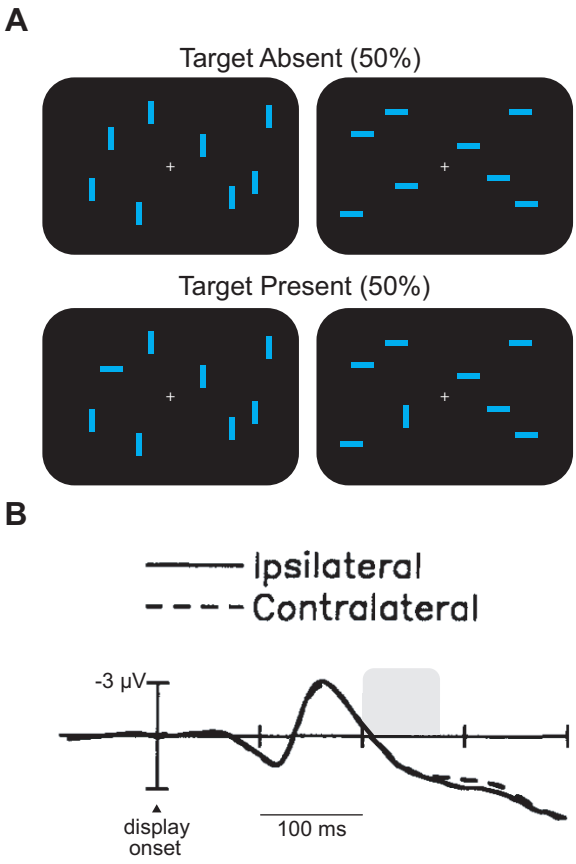

Figure 1. Testing the spatial filtering hypothesis. (**A**) The four stimulus displays used in Luck and Hillyard's (1994) singleton detection experiment and in the present study. (**B**) ERP results from Luck and Hillyard's (1994) singleton detection experiment. The shaded region denotes the time window used to measure the N2pc mean amplitude. Reprinted with permission.

obtained from healthy individuals; Luck, Fuller, Braun, Robinson, Summerfelt, & Gold, 2006; Luck & Gold, 2008).

Much of the evidence for the spatial filtering hypothesis comes from experiments designed to either permit the hypothetical filtering process or to discourage it from being implemented (Luck & Hillyard, 1994a). The general approach is simple: The N2pc should be present whenever filtering is possible and should be absent whenever filtering is unlikely. In one experiment, filtering was discouraged by randomly switching the orientation of the target with that of the distractors across trials (Luck & Hillyard, 1994a, Experiment 2; see Figure 1A). When the features of a singleton and the surrounding distractors vary unpredictably, it is assumed that participants strategically search for a discontinuity in the display rather than for an item possessing a specific feature. This strategy has been labelled the *singleton detection mode* (Bacon & Egeth, 1994). Luck and Hillyard hypothesized that distractor suppression would be minimized in singleton detection mode because it would interfere with the detection of a discontinuity. On these grounds, the N2pc was predicted to be absent in the singleton-detection task. Consistent with this prediction, the observed contralateral-ipsilateral difference was reported to be small and statistically nonsignificant (0.2 μV; $p > .15$), leading Luck and Hillyard to conclude that the N2pc is absent when the task discourages spatial filtering (see also Luck, 2012). The results also indicate that singleton detection does not require the selection processes that give rise to the N2pc (cf. Luck & Ford, 1998).

In the decades that followed Luck and Hillyard's (1994a) seminal work, very few studies have sought to replicate their null result or to confirm the conclusion that the N2pc is absent in singleton detection tasks. In one study, Mazza, Turatto, and Caramazza (2009) reported that colour singletons elicited an N2pc in both fixed-feature and variable-feature conditions.

However, participants were required to discern whether the target possessed a notch on the left or right side in this task, and so filtering may have occurred during this feature-based selection process. It is also possible that the alternation of fixed-feature and variable-feature blocks led to some carry-over of attention processes across block types. Another study that involved an orientation singleton detection task found that the N2pc was absent for small set sizes (2, 4, 5, or 6 items) but was present for larger set sizes (10, 25, 45, 48, or 49 items; Schubö, Schröger, & Meinecke, 2004). The absence of N2pc for small set sizes was interpreted as supporting the hypothesis that singleton detection can be accomplished without attention, whereas the presence of N2pc for larger set sizes was taken as evidence for a shift in processing mode (cf. Meinecke and Donk, 2002). Although Schubö and colleagues did not make any conclusion as to whether the N2pc reflected distractor suppression or target enhancement, the presence of the N2pc in their singleton detection tasks would seem to be inconsistent with predictions stemming from the spatial filtering hypothesis. It is conceivable, however, that a singleton might automatically trigger a top-down filtering process when its bottom-up salience is great enough to survive interference caused by surrounding items (Luck, 2012).

In addition to the infrequent observations of N2pc in singleton-detection tasks (Mazza et al., 2009; Schubö et al., 2004), two related findings provide some evidence against the distractor-filtering hypothesis of N2pc. If distractor filtering triggers a posterior contralateral negativity, one might predict this negativity to show up contralateral to a distractor rather than to a target when the display contains just one target and one distractor on opposite sides of fixation. However, the N2pc shows up contralateral to the target, not the distractor, under such conditions (Eimer, 1996). And when the target is placed on the vertical meridian and the distractor luminance is reduced (and matched to the background), a posterior positivity—not a negativity—

is observed contralateral to the distractor (Hickey, Di Lollo, & McDonald, 2009). These findings indicate that target selection might trigger contralateral negativities (such as the N2pc) and that distractor filtering might trigger a component called the distractor positivity (P_D; Hickey et al., 2009).

The main objective of the present study was to determine whether the detection of an orientation singleton elicits the N2pc using 8-item displays similar to those in Luck and Hillyard's (1994a) singleton detection experiment (Experiment 2). More specifically, we aimed to test Luck's (2012) hypothesis that "filtering should be minimized in this task, and little or no N2pc activity should be observed" (p. 349). Based on this rationale, a positive result yielding a moderate-to-large effect ($d \geq 0.5$) would cast doubt on the spatial filtering hypothesis and would show that the attentional process(es) driving the N2pc are involved in singleton detection as well as fixed-feature search tasks. At the outset, we surmised that the jump from an 8-item display to a 10-item display (as used by Schubö et al., 2004, Experiment 2) is unlikely to be a deciding factor in determining whether singleton detection would trigger an N2pc. Instead, we focused on competing statistical considerations stemming from the two preceding studies. On the one hand, by not correcting for multiple comparisons, Schubö et al. may have made a Type I error in concluding that the N2pc was statistically significant for their 10-item display (with $P = 0.037$ and four t-tests, the N2pc would not have survived correction for multiple comparisons). In addition, Schubö and colleagues switched to a later measurement window (250–350 ms) without a clear justification for doing so (although it is possible the N2pc occurs later when the target features are variable than when they are fixed; cf. Eimer, Kiss, & Cheung, 2010). On the other hand, Luck and Hillyard may have made a Type II error in concluding that the N2pc was absent

in their study. A cursory power analysis reveals that one would need a sample size of 156 participants to detect a small effect ($d = 0.20$) with reasonable power (0.71).

Methodologically, we made five changes to Luck and Hillyard's (1994a) experimental procedures and analytical approach to increase signal size and gain statistical power. First, we ran 600 more trials per participant to reduce noise in the ERPs. Second, we specifically looked at ERPs elicited by lower-field targets, because the N2pc is known to be larger in the lower field than in the upper field (Luck et al., 1997). Third, whereas Luck and Hillyard measured the mean amplitude of the N2pc in a 200–275 ms time window, we measured the N2pc in two additional ways: (i) as the mean amplitude in a 250–350 ms time window, and (ii) as the signed negative area from 200–350 ms. The 250–350 ms measurement window was selected *a priori* because it matched the timing of a small, N2pc-like negativity seen in Luck and Hillyard's waveforms (see Figure 1B) and was the measurement window used by Schubö et al. (2004). The wide window used for signed area measurement was selected to span the measurement windows used across the two aforementioned studies and to avoid "cherry picking" a window based on the observed data (Luck, 2012). Fourth, we measured N2pc at electrodes PO7 and PO8, where it is typically largest, rather than at other nearby occipital (O1 and O2) and parietal (P7 and P8) electrodes. Finally, we increased the sample size from 12 to 26 participants. This sample size was selected based on a power analysis that was predicated on the assumption that a lower-field N2pc would be, at minimum, a moderate-sized effect ($d \geq 0.50$; power ≥ 0.72). In addition to the main N2pc analyses, secondary analyses were performed to discover other electrophysiological correlates of singleton detection.

2. Method

The Research Ethics Board at Simon Fraser University (SFU) approved the research protocol used in this study. All experimental procedures were performed in accordance with guidelines and regulations outlined by SFU and the Natural Sciences and Engineering Research Council of Canada.

2.1. Participants

Thirty-one undergraduate students from Simon Fraser University participated after giving informed consent. Participants were given course credit as part of a departmental research participation system. All participants reported normal or corrected-to-normal visual acuity and had normal color vision (tested with Ishihara color plates). Data from five participants were excluded from the analysis because of excessive ocular artifacts (>25% of the trials in one or both conditions were rejected due to horizontal eye movements or blinks). Of the remaining 26 participants, 15 were female and 25 were right-handed. Their mean age was 21.6 years.

2.2. Apparatus

The experiment was conducted in an electrically shielded chamber dimly illuminated by DC-powered LED lighting. Visual stimuli were presented on an LCD monitor running at 120 Hz and viewed from a distance of 57 cm. Stimulus presentation was controlled by Presentation (Neurobehavioral Systems, Inc., Albany, CA) from a Windows-based computer. EEG was recorded using custom software (Acquire) from a second Windows-based computer, using a 64-channel A-to-D board (PCI 6071e, National Instruments, Austin, TX) connected to a high input impedance EEG amplifier system (SA Instruments, San Diego, CA). The stimulus-control and acquisition computers were situated outside of the testing chamber.

2.3. Stimulus and Procedure

Each stimulus display consisted of a small, white fixation cross (0.3° × 0.3°; 0.3 cd/m^2) positioned at the middle of the display and eight blue bars (0.3° × 1.0°; x = 0.20, y = 0.35, 17.5 cd/m^2) appearing within a 10.7° × 7.9° region around fixation. The coordinates of each bar were chosen randomly, subject to the following constraints: four bars were presented on each side of fixation; no bar overlapped another bar; no bar overlapped one of the invisible meridians (horizontal or vertical). Target-absent displays contained eight horizontal bars or eight vertical bars, and on target-present displays, one of the eight distractor bars was replaced with an orientation singleton that was rotated 90° with respect to the distractors. The four display types, illustrated in Figure 1A, appeared randomly and with equal probability within each block of trials. Stimulus duration was 750 ms, and the stimulus onset asynchrony varied randomly between 1,350 ms and 1,650 ms. Participants held a gamepad with both hands and indicated the presence or absence of the target by pressing either the left or right shoulder button with one of their index fingers. The stimulus-response mapping was counter-balanced across participants. At the outset, participants were instructed to maintain eye fixation on the central cross and were given at least one block of practice to learn the task. The entire experiment was comprised of 35 blocks of 40 trials, with participant-controlled rest periods between blocks.

2.4. Behavior

Median reaction times (RTs) were computed for target-absent and target-present trials, separately for each participant. Trials on which the participant responded incorrectly, too quickly (RT < 100 ms), or too slowly (RT > 1,350 ms) were excluded from the analysis. Median RTs for target-present trials were further subdivided into upper-field target and lower-field target trials. Finally, median RTs were derived for subsets of target-present trials based on whether the

preceding trial contained a target with the same orientation (i.e., repeat-orientation trials) or opposite orientation (i.e., change-orientation trials) to determine whether responses were faster when the display configuration repeated across successive trials, an effect known as priming of pop-out (Maljkovic & Nakayama, 1994).

2.5. Electrophysiology

2.5.1. Recording and pre-processing. Electroencephalographic (EEG) signals were recorded from 25 sintered Ag-AgCl electrodes positioned at standard 10-10 sites (FP1, FPz, FP2, F7, F3, Fz, F4, F8, T7, C3, Cz, C4, T8, P7, P3, Pz, P4, P8, PO7, POz, PO8, O1, Oz, O2, and M1). An additional pair of electrodes placed 1 cm lateral to the external canthus of each eye was used to monitor the horizontal electrooculographic (EOG) activity. During recording, all EEG signals were referenced to an electrode positioned on the right mastoid (M2), with the ground electrode positioned over the midline frontal scalp (site AFz). EEG and EOG signals were amplified with a gain of 20,000 within a passband of 0.01–100 Hz (2-pole Butterworth filters) and were digitized at 500 Hz. A semi-automatic procedure was performed to remove epochs of EEG that were contaminated by eye movements, blinks, or amplifier blocking (for detail, see Green, Conder, & McDonald, 2008). Artifact-free data were then used to create averaged ERP waveforms, which were digitally low-pass filtered (half-power cut-off at 30 Hz) to remove high-frequency activity. Each EEG channel was digitally re-referenced to the average of the left and right mastoids. After discarding data from five participants due to excessive ocular artifacts (> 25% of trials), the averaged event-related HEOG deflections did not exceed 2 μV for any individual participant.

For each participant, ERPs elicited by search displays containing a target in the left or right visual field were combined in such a way as to produce waveforms recorded contralateral and

ipsilateral to the target. This was done for the "raw" target-present ERPs and for difference waves constructed by first subtracting target-absent ERPs from the left-visual-field target ERPs and from the right-visual-field target ERPs (herein called present-minus-absent difference waves). Contralateral-minus-ipsilateral difference waveforms were computed for target-present displays by subtracting ipsilateral waveforms from corresponding contralateral waveforms, separately for each pair of lateral electrodes (e.g., PO7 and PO8). Negative voltages were plotted upward so that the N2pc would appear in these difference waveforms as an upward deflection.

2.5.2. Analysis. All N2pc measurements were taken from contralateral-ipsilateral difference waves recorded at electrodes PO7 and PO8. Except where noted, all statistical tests were performed with two tails. To replicate and extend previous measurement approaches, the magnitude of the N2pc was quantified as the mean amplitude within a 200–275-ms window (Luck & Hillyard, 1994a), as the mean amplitude within a 250–350-ms measurement window (Schubö et al., 2004), and as the signed negative area within a 200–350-ms window that spanned both mean-amplitude windows. We first conducted one-sample t-tests to determine whether the mean amplitudes within the early and late measurement windows differed significantly from zero microvolts. To be consistent with previously published studies, these two tests were performed using data from all target-present trials. Next, data from upper-field and lower-field targets were separated to determine whether (i) the mean N2pc amplitude in each measurement window was more negative in the lower field than in the upper field (paired t-tests), and (ii) the mean N2pc amplitude for lower-field targets was statistically different from zero (one-samples t-test). To reduce the number of statistical tests performed, we did not seek to determine whether upper-field targets elicited the N2pc.

Following the mean-amplitude tests, the signed negative areas within the wide measurement window were assessed for the presence of an N2pc and for magnitude differences between upper- and lower-field targets. Because noise contributes to the measured signed area even in the absence of a signal, the traditional statistical approach (of evaluating the measure against a mean of zero, using variability across participants) was supplanted by a nonparametric permutation approach (Sawaki et al., 2012). Briefly, the target-present display events were randomly re-coded for target lateralization (left, right) to eliminate lateralized ERP signals and enable estimation of noise within the measurement window. This re-coding process was done for each subject's data 500 times to yield 500 different grand-averaged ERPs, which were then used to construct a distribution of signed negative area values that would be expected to arise from noise alone if the null hypothesis were true. The observed grand-average N2pc would be considered statistically present if the measured signed area fell beyond the 95th percentile of the noise distribution. The p-value for this permutation test was calculated using the following equation (Phipson & Smyth, 2010; see also Gaspelin & Luck, 2018):

$$P = \frac{1 + (number\ of\ permuted\ values\ \geq\ observed\ area)}{1 + total\ number\ of\ permutations}$$

Because multiple, conceptually overlapping tests were performed on the various N2pc measures, we decided a priori to base our conclusions on the results of the signed area test of the lower-field N2pc, because we predicted that the N2pc would be largest there and because we hypothesized that the N2pc would appear later than the 200–275 ms window in a singleton-detection task with a relatively sparse 8-item array (note 200–275 ms window was originally based on results of a fixed-feature search task; Luck & Hillyard, 1994a, 1994b).

Three additional tests were planned to further assess the N2pc (all paired t-tests). First, N2pc onset latency was measured as the latency within the broader measurement window (200–350

ms) at which each N2pc first reached 25% of its peak amplitude. This was done primarily to compare the time at which the N2pc emerged with the timing of an overlapping occipital positivity (described in the next paragraph) using a conventional jackknife approach (Miller, Patterson, & Ulrich, 1998). Second, contralateral-ipsilateral difference waves were computed separately for repeat- and change-orientation trials. Based on previous studies of inter-trial effects, we predicted that RTs would be faster on repeat-orientation trials than on change-orientation trials (Maljkovic & Nakayama, 1994) and that any observable N2pc would occur earlier for repeat-orientation trials than for change-orientation trials (Christie, Livingstone, & McDonald, 2015; Eimer, Kiss, & Cheung, 2010). Because of the reduction of the numbers of trials contributing to the N2pc averages and the concomitant reduction in the signal-to-noise ratio (vs. the all-targets N2pc), it was decided a priori to test for a difference in the timing of N2pc latencies between the two trial types using the time at which the N2pc first reached 50% of its peak amplitude, again using the jackknife approach. Third, we re-computed ERPs separately for fast-response and slow-response trials (determined using a median split of RTs; see McDonald, Green, Jannati, & Di Lollo, 2013), on the hypothesis that the N2pc (and other signs of singleton detection; see next paragraph) might be larger or earlier for fast-response trials. Signed area measures were used to examine differences in N2pc magnitude. Again, because this median-split analysis necessarily reduces the number of trials in the N2pc averages, a 50% peak amplitude latency was also used in the assessment of N2pc timing across the two subsets of trials.

Following the N2pc analyses, three exploratory sets of analyses were performed to determine what other ERP components might be evident in the singleton detection task. The first targeted a lateralized N1—the N1pc—that has been associated with an initial stage of spatial processing of unilateral stimuli (Verleger, vel Grajewska & Jaśkowski, 2012; Wascher & Beste,

2010a, 2010b). The N1pc was measured as the mean amplitude within a 50-ms time window centered on the posterior N1 peak (150–200 ms). The second exploratory test targeted an occipital positivity that has been reported in a few previous studies (Luck & Hillyard, 1990; 1994b; Schubö et al., 2004). The previously reported occipital positivities were measured in the time range of the P3b, but pilot data from our lab indicated that an earlier occipital positivity might appear when the target and nontarget features swap unpredictably across trials (unpublished observation). Therefore, we first set out to characterize the timing of this earlier occipital positivity—which we call the singleton detection positivity (SDP)—and then used this information to select appropriate time windows for measurement of mean amplitudes (here and in subsequent studies). All SDP measurements were taken from target-present minus target-absent difference waves to reduce overlap from components visible in the "raw" ERP waveforms (including P3b). Onset latency was measured as the first time point at which the SDP reached 25% of its peak amplitude, and differences in onset latencies (e.g., between contralateral and ipsilateral electrodes) were tested statistically using the jackknife approach. The mean amplitude of the SDP was then measured within four consecutive 50-ms time windows starting just before the measured onset latency (e.g., 201–250 ms if onset measured to be within that 50-ms interval), separately at contralateral and ipsilateral electrodes (PO7/8) to help establish the appropriate measurement window in future studies. Each of the four mean-amplitude measurement windows was tested against the significance threshold of 0.0063 to limit the familywise error rate to 0.05 (with 8 two-tailed tests).

In the third and final set of exploratory analyses, we set out to determine whether there were any linear correlations between different ERP measures of interest or between select ERP measures of interest and RT. For the inter-component correlations, we computed Pearson

correlation coefficients for the magnitude of N2pc (measured as the signed negative area within the 200–350 ms window) and each of the following: P1 mean amplitude (75–125 ms; collapsed across contralateral and ipsilateral electrodes), N1 mean amplitude (150–200 ms; collapsed across contralateral and ipsilateral electrodes), the N1pc (150-200 ms), and the SDP recorded from the ipsilateral electrode (to avoid picking up the N2pc over the contralateral scalp). The magnitude of the SDP was measured as the mean amplitude in a window within which the SDP was found to be significant (which turned out to be 200–400 ms). Pearson correlation coefficients were also computed between RT and each of the following ERP measures: N2pc area (measured as above), N2pc onset latency (25% fractional peak latency), SDP mean amplitude (as defined above), and SDP onset latency (25% fractional peak latency). Inter-component and RT correlations were separately measured across all participants or all Jackknife sub-averages and were tested for significance using conventional parametric methods, with Bonferroni correction for multiple comparisons (per-test $\alpha = 0.05/4$).

3. Results

3.1. Behavior

There was no RT difference between target-present trials and target-absent trials (536 ms vs. 531 ms, respectively), $t = .98$, $P = 3345$, or between upper-field targets and lower-field targets (534 ms vs. 538 ms, respectively), $t = 1.38$, $P = 0.1795$. Responses were faster on repeat-orientation trials than on change-orientation trials (550 ms vs. 569 ms, respectively), $t = 6.78$, $P < 0.0001$, $d = 0.36$, indicating that priming of pop-out occurred (Maljkovich & Nakayama, 1994).

3.2. Electrophysiology

As Figure 2 shows, our occipitally recorded ERPs looked similar to those obtained by Luck and Hillyard (1994, Experiment 2) at somewhat more lateral electrode sites. ERPs recorded over the contralateral and ipsilateral occipital scalp consisted of the usual P1 (peaking ~110 ms) and N1 (peaking ~170 ms) deflections, followed by a longer-lasting positive-going slow wave. Notably, in the present study as well as in Luck and Hillyard's study, the contralateral waveform is slightly more negative than the ipsilateral waveform starting approximately 250 ms and continuing for roughly 100 ms. When measured as the mean voltage between 200 ms and 275 ms post-stimulus, the small (-0.18 μV) contralateral negativity, representing the initial phase of the N2pc, was not statistically significant, $t = 1.39$, $P = 0.1800$. However, when measured as the mean voltage between 250 ms and 350 ms post-stimulus, the N2pc grew in magnitude (to -0.49 μV) and became statistically significant, $t = 2.95$, $P = 0.0069$, $d = 0.58$. The grand-average signed negative area (54.9 μV*ms) within the 200–350 ms measurement window was also highly significant, $P = 0.0020$ (Figure 3A). The preceding N1pc (-.16 μV, measured over 150–200 ms) was marginally significant, $t = 2.03$, $P = 0.0529$, $d = 0.40$. The residual HEOG deflection in the grand-averaged HEOG waveform was less than -0.46 μV and began roughly 282 ms after display onset, which indicates that the larger and earlier-onsetting N2pc could not be due to volume conduction of saccade-induced activity (see Figure 2B).

Figure 4 shows the lateral occipital ERPs elicited by displays containing upper-field targets and lower-field targets. As predicted, the N2pc appeared to be larger for lower-field targets. This magnitude difference was confirmed statistically in the early (200–275 ms) mean-amplitude measurement window, $t = 3.33$, $P = 0.0027$, $d = 0.82$, as well as in the late (250–350 ms) mean-amplitude window, $t = 4.77$, $P < 0.0001$, $d = 0.88$. The N2pc triggered by lower-field targets was

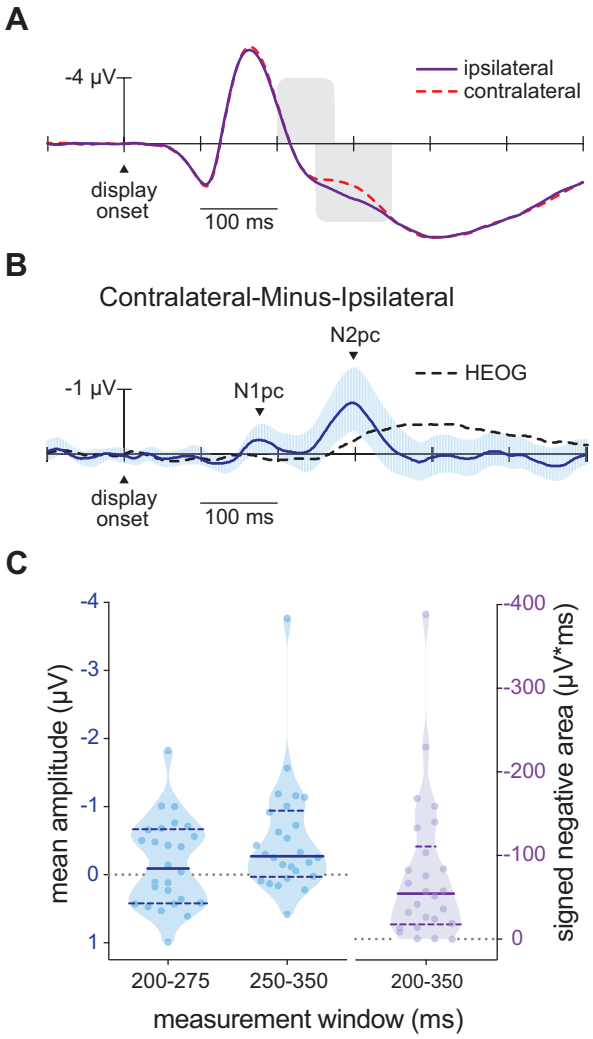

Figure 2. Grand-averaged ERPs recorded over the lateral occipital scalp (electrodes PO7 and PO8). (**A**) Waveforms recorded contralateral and ipsilateral to target singletons appearing in the upper or lower visual field (all target-present trials). The shaded regions above and below the x-axis depict the time windows used to measure the N2pc mean amplitude (200–275 ms and 250–350 ms). (**B**) The contralateral-minus-ipsilateral difference wave corresponding to the ERP waveforms in panel A. The light blue vertical bars correspond to the 95% confidence intervals at each sample point in the plotting window. The residual HEOG deflection is plotted alongside the difference wave to contrast its latency and magnitude with that of the N2pc. (**C**) Violin plots showing the median, quartiles, and individual-participant data points for the mean amplitude measured in the 200–275 ms window (left), the mean amplitude measured in the 250–350 ms window (middle), and the signed negative area measured in the 200–350 ms window (right).

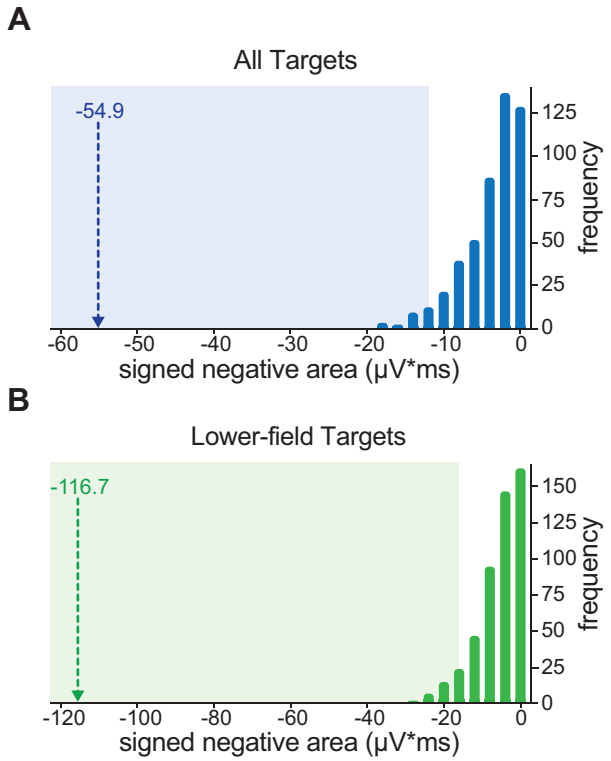

Figure 3. Permutations tests of the signed negative areas within the time interval of the N2pc (200–350 ms, post-stimulus). The vertical bars indicate the distributions of signed negative areas of the scrambled grand-averages (i.e., the noise distributions). The shaded regions indicate the signed negative areas above the 95th percentile from the noise distributions, and the vertical dashed lines indicate the measured signed negative areas from the original, unscrambled datasets. (**A**) Test for all-target N2pc. (**B**) Test for lower-field N2pc.

found to be present in both mean-amplitude measurement windows (early: $t = 2.51$, $P = 0.0188$, $d = 0.50$; late: $t = 4.15$, $P = 0.0003$, $d = 0.81$). Signed negative area measures confirmed the presence of N2pc for lower-field targets (-116.7 μV*ms; $P = 0.0020$; see Figure 3B) as well as the larger N2pc for lower-field targets than for upper-field targets, $t = 4.76$, $P < 0.0001$, $d = 1.01$. The magnitudes of residual HEOG deflections (measured as the mean amplitudes within a 350–-400-ms window) associated with upper- and lower-field targets were found not to differ, $t = 0.057$, $P = 0.9550$, indicating that the larger N2pc to lower-field targets was not associated with undetected saccades. To estimate the internal reliability of the N2pc signed area measure, we

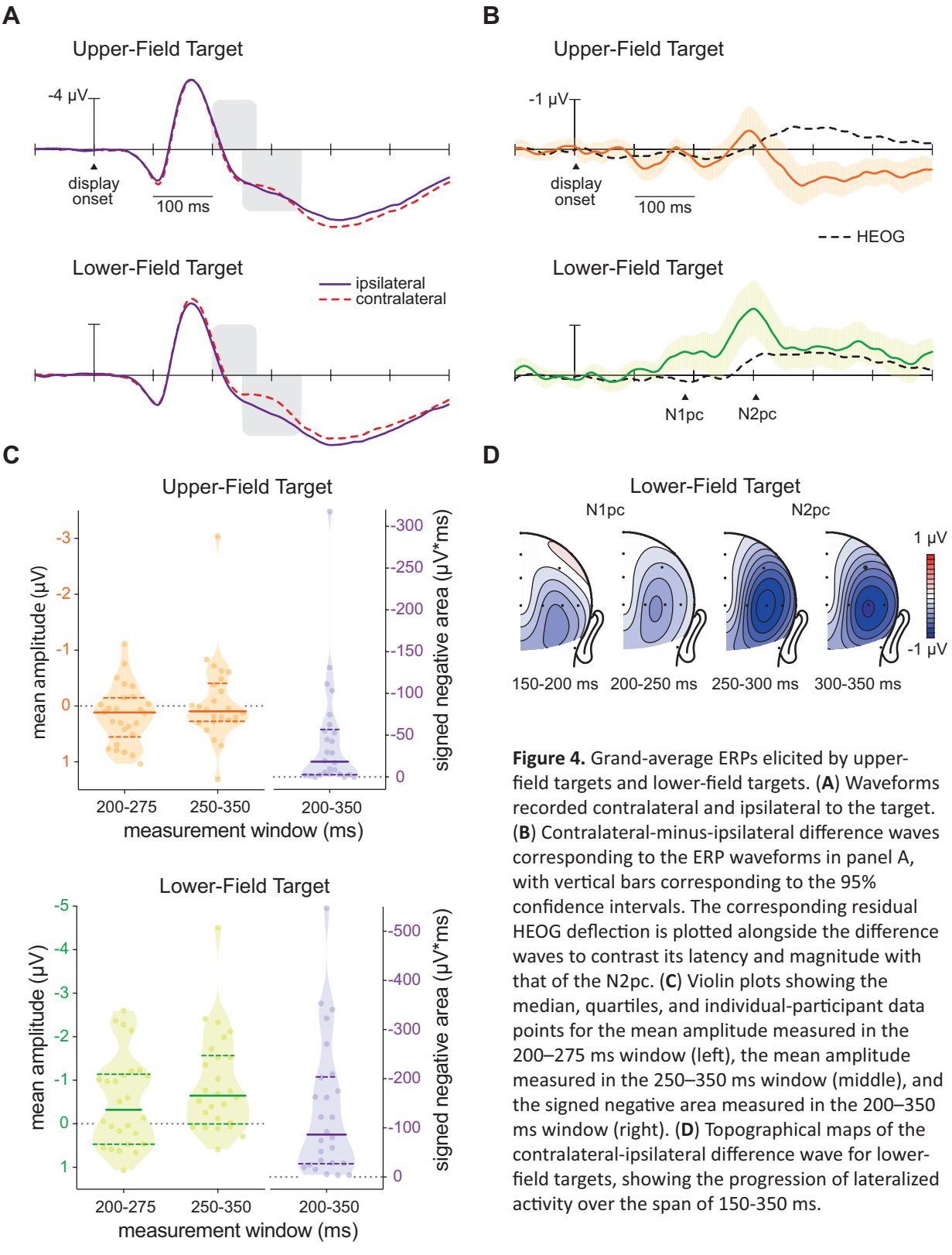

Figure 4. Grand-average ERPs elicited by upper-field targets and lower-field targets. (**A**) Waveforms recorded contralateral and ipsilateral to the target. (**B**) Contralateral-minus-ipsilateral difference waves corresponding to the ERP waveforms in panel A, with vertical bars corresponding to the 95% confidence intervals. The corresponding residual HEOG deflection is plotted alongside the difference waves to contrast its latency and magnitude with that of the N2pc. (**C**) Violin plots showing the median, quartiles, and individual-participant data points for the mean amplitude measured in the 200–275 ms window (left), the mean amplitude measured in the 250–350 ms window (middle), and the signed negative area measured in the 200–350 ms window (right). (**D**) Topographical maps of the contralateral-ipsilateral difference wave for lower-field targets, showing the progression of lateralized activity over the span of 150-350 ms.

sorted alternating targets into two separate averaging bins, constructed ERPs for the two halves of trials for each participant, measured the signed negative area within the N2pc time interval for each split-half contralateral-minus-ipsilateral difference wave, and computed the Spearman-Brown coefficient between the split-half N2pc area measures across participants. The resulting split-half reliability was 0.96. Topographical mapping of the contralateral-ipsilateral difference waveforms confirmed that the lateralized negativity was largest at PO7/8 (Figure 4D), consistent with prior reports of the N2pc scalp distribution (Luck, 2012).

Like the N2pc, the N1pc was larger for lower-field targets than for upper-field targets (-0.37 μV vs. 0.06 μV, respectively; $t = 2.90$, $P = 0.0076$, $d = 0.79$) and was found to be present for targets in the lower field, $t = 2.74$, $P = 0.0111$, $d = 0.54$ (Figure 4).

Figure 5 shows the contralateral-ipsilateral difference waveforms for repeat-orientation and change-orientation trials (panel A) and for fast-response and slow-response trials (panel B). In line with the RT effect, the difference in N2pc latency between repeat-orientation and change-orientation trials was marginally significant, with a shorter latency for repeat-orientation trials than for change-orientation trials (256 ms vs. 276 ms, respectively), $t = 2.00$, $P = 0.0564$, $d = 0.44$. No difference in N2pc area was found, $t = 0.85$, $P = 0.4018$. These results suggest that inter-trial priming of pop-out facilitated detection of the target singleton in the present study. The RT-based median-split analysis revealed that the N2pc was earlier (253 ms vs. 271 ms), but not significantly larger (-98.0 μV*ms vs. -70.1 μV*ms), on fast-response trials than on slow-response trials (latency: $t = 2.08$, $P = 0.0481$, $d = 0.39$; area: $t = 1.49$, $P = 0.1500$). Interestingly, an N1pc was evident on both repeat- and change-orientation trials, $ts \geq 2.60$, $Ps \leq 0.0156$, $ds \geq 0.50$, but no difference in amplitude was found between the two types of trials, $t = 0.03$, $P = 0.9739$. An N1pc was also evident on fast-response trials, $t = 2.64$, $P = 0.0142$, $d = 0.56$, but

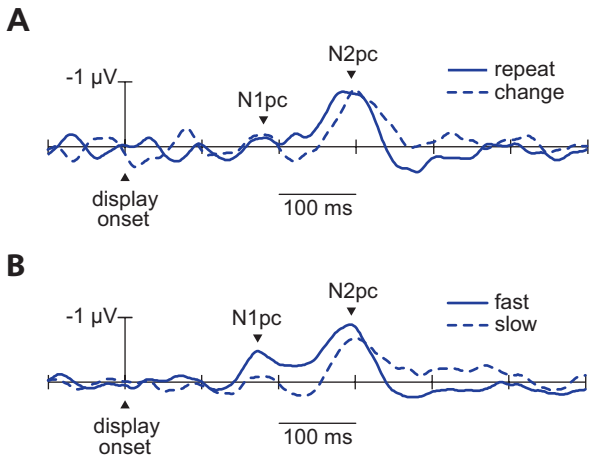

Figure 5. Contralateral-minus-ipsilateral difference waves for select subsets of trials. (**A**) Difference waves for repeat-orientation trials (target preceded by same-orientation target) and change-orientations trials (target preceded by opposite-orientation target). (**B**) Difference waves for targets on fast-response trials and slow-response trials divided based on the median RTs of individual participants.

not on slow-response trials, $t = 0.62$, $P = 0.5389$.

Figure 6 illustrates ERPs elicited by target-present and target-absent displays over frontal, central, parietal, and occipital scalp sites (Figure 6A) along with present-minus-absent difference waves recorded over the contralateral and ipsilateral occipital scalp (relative to target location; Figure 6B). Unsurprisingly, both target-present and target-absent displays elicited the usual P3b that was maximal around Cz and Pz (Figure 6A, C). The P3b appeared to be larger for target-absent trials than for target- present trials at midline frontal, central, and parietal sites, but over the lateral occipital scalp, the ERPs were more positive for target-present trials than for target-absent trials. We refer to this occipital positive difference as the SDP (singleton detection positivity) to differentiate it from the P3b and other common variants of the P3 family of components. The bilaterally symmetrical SDP appeared to begin roughly 200 ms after onset of the search array and roughly 30 ms before the onset of the lateralized N2pc (Figure 6B). SDP onset latencies were found to be 219 ms and 218 ms at contralateral and ipsilateral electrodes,

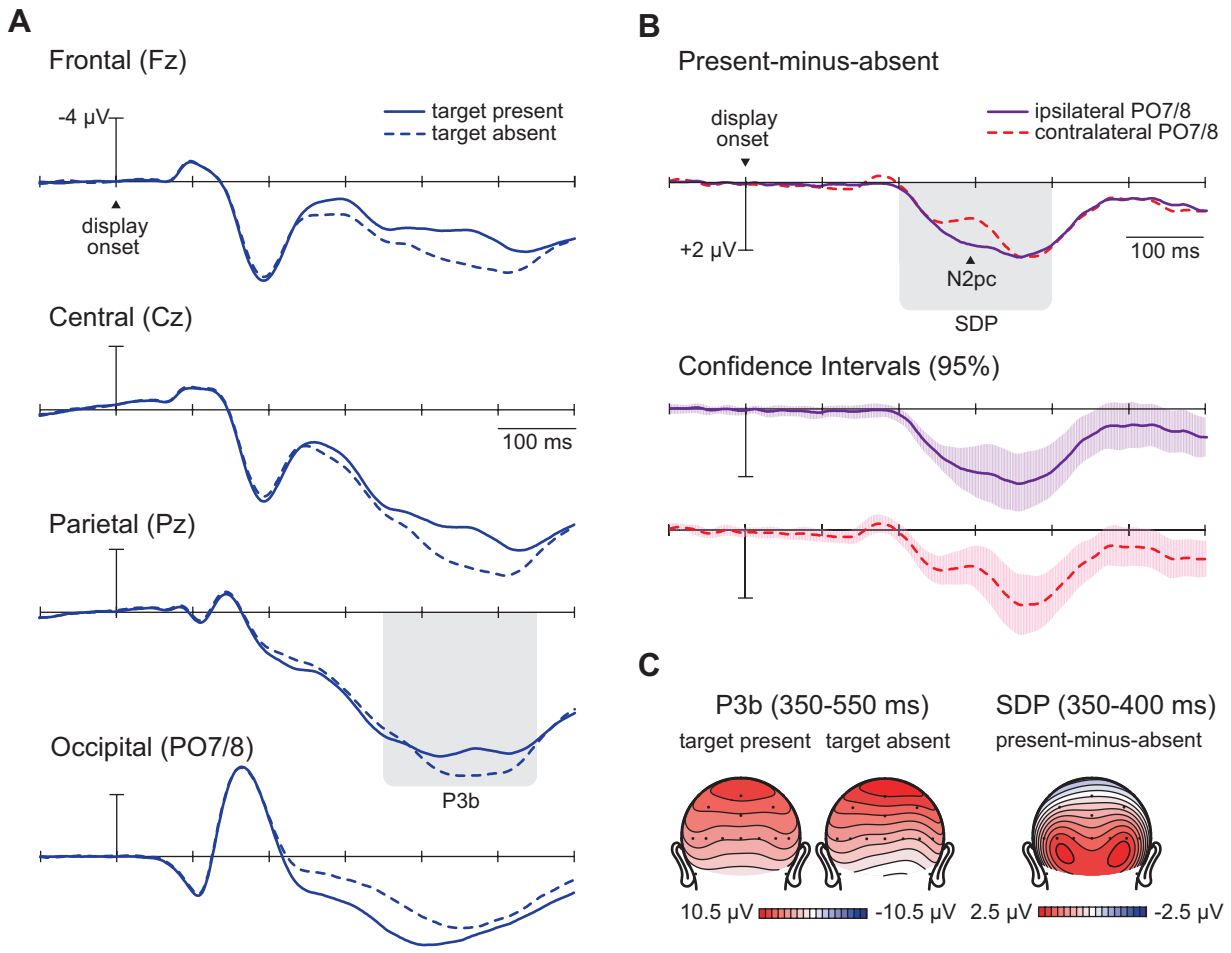

Figure 6. Isolation of singleton-related processing. (**A**) Grand-averaged ERP waveforms elicited by target-present and target-absent display, recorded over the midline frontal, central, and parietal (electrodes Fz, Cz, and Pz) scalp, as well as the lateral occipital (averaged across electrodes PO7 and PO8) scalp. The shaded region denotes the time range and scalp location of maximal P3b activity. (**B**) Upper half panel shows target-present-minus-target-absent difference waves recorded at contralateral occipital (contra-PO7/8) and ipsilateral occipital (ipsi-PO7/8) scalp. The shaded region denotes the time range of maximal SDP activity. Lower half panel shows blue and red vertical bars corresponding to the 95% confidence intervals of contralateral and ipsilateral SDP, respectively. (**C**) On the left, topographical maps of the P3b (350–550 ms) elicited by target-present displays and target-absent displays. Left- and right-target ERPs were combined to produce the target-present maps, with ipsilateral and contralateral electrodes positioned on the left and right sides of the head, respectively. The target-absent maps show the original electrode montage with left and right electrodes positioned on the left and right sides of the head, respectively. On the right, topographical maps of the present-minus-absent difference waves, with ipsilateral and contralateral electrodes (relative to target) positioned over the left and right sides of the head, respectively. At 350-400 ms, the SDP can be seen over the lateral occipital scalp.

respectively (no significant difference; $t = 0.14$, $P = 0.891$). Each of these onset latencies was found to be statistically earlier than the onset latency of the N2pc (252 ms; contralateral SDP vs. N2pc: $t = 2.28$, $P = 0.0311$, $d = 0.78$; ipsilateral SDP vs. N2pc: $t = 3.27$, $P = 0.0031$, $d = 0.89$; all measured as 25% fractional peak latency). Confidence intervals (95%) around the grand-averaged difference waves corroborated this finding; namely, the SDP confidence intervals became fully positive at 212 and 206 ms over the contralateral and ipsilateral scalp, respectively (Figure 6B), whereas the N2pc confidence intervals only became fully negative at 262 ms post-stimulus (Figure 2B). The confidence intervals also show that both the contralateral (212–464 ms) and ipsilateral (206–458 ms) SDP lasted longer than the N2pc (262–322 ms). SDP mean amplitudes were significantly different from zero in all four 50-ms measurement windows (201–250 ms, 251–300 ms, 301–350 ms, and 351–400 ms) over the contralateral scalp, $ts \geq 4.05$, $Ps \leq 0.0004$, $ds \geq 0.79$, and over the ipsilateral scalp, $ts \geq 4.82$, $Ps \leq 0.0001$, $ds \geq 0.95$. The split-half reliability of SDP was 0.92 on both the contralateral side and the ipsilateral side (when measured as the mean amplitude in the 200–400 ms interval).

Finally, as illustrated in Figure 7, the magnitude of the N2pc was found to correlate positively with the magnitudes of the posterior N1 component, $r = 0.66$, $P = 0.0003$, with the N1pc component, $r = 0.58$, $P = 0.0021$, and marginally with the ipsilateral SDP, $r = 0.47$, $P = 0.0154$ (the polarities of the signed areas were ignored so that a positive correlation coefficient would indicate that as one component increased in absolute magnitude, the other did as well). To help visualize these relationships, we sorted participants into two groups based whether their N2pc was smaller or larger than the median magnitude and re-plotted the contralateral and ipsilateral ERPs from lateral occipital electrodes (PO7, PO8). This was done using the "raw" target-present ERPs, the contralateral-minus-ipsilateral difference waves, and the target-present-

minus-target-absent difference waves to visualize the N2pc-N1 relationship, the N2pc-N1pc relationship, and the N2pc-SDP relationship, respectively. The resulting waveforms show that the bilateral N1, N1pc, and SDP were larger for the large-N2pc group than it was for the small-N2pc group. The magnitude of the posterior P1 did not correlate with that of the N2pc, $r = 0.05$, $P = 0.7970$. RTs were found to correlate with the onset latency of the SDP, $r = 0.55$, $P = 0.0035$, but not with SDP amplitude, N2pc magnitude, or N2pc onset latency, $rs \leq 0.119$, $Ps \geq 0.564$).

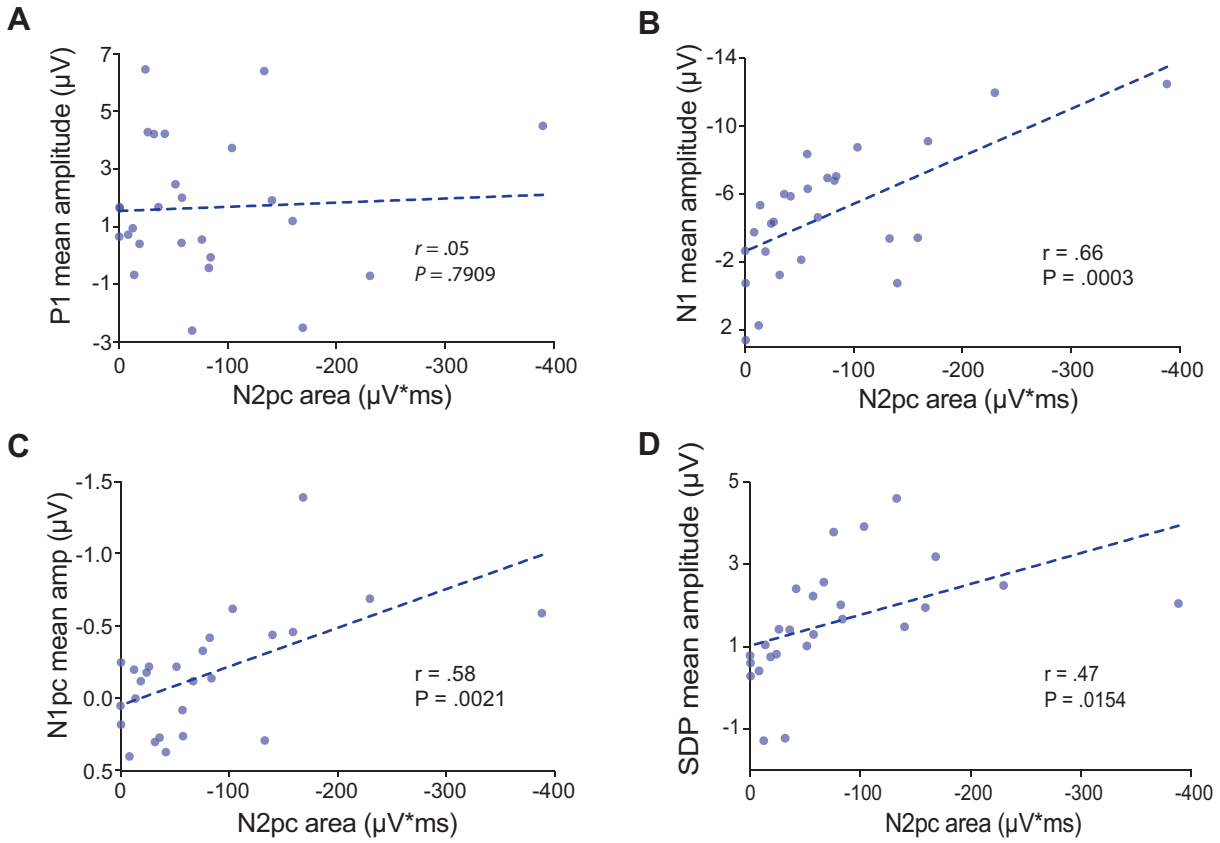

Figure 7. Relationships between the magnitudes of the N2pc and the posterior P1, posterior N1, N1pc, and singleton detection positivity (SDP). (**A**) Scatterplot of N2pc area and P1 mean amplitude. (**B**) Scatterplot of N2pc area and N1 mean amplitude. (**C**) Scatterplot of N2pc area and N1pc mean amplitude. (**D**) Scatterplot of N2pc area and SDP mean amplitude.

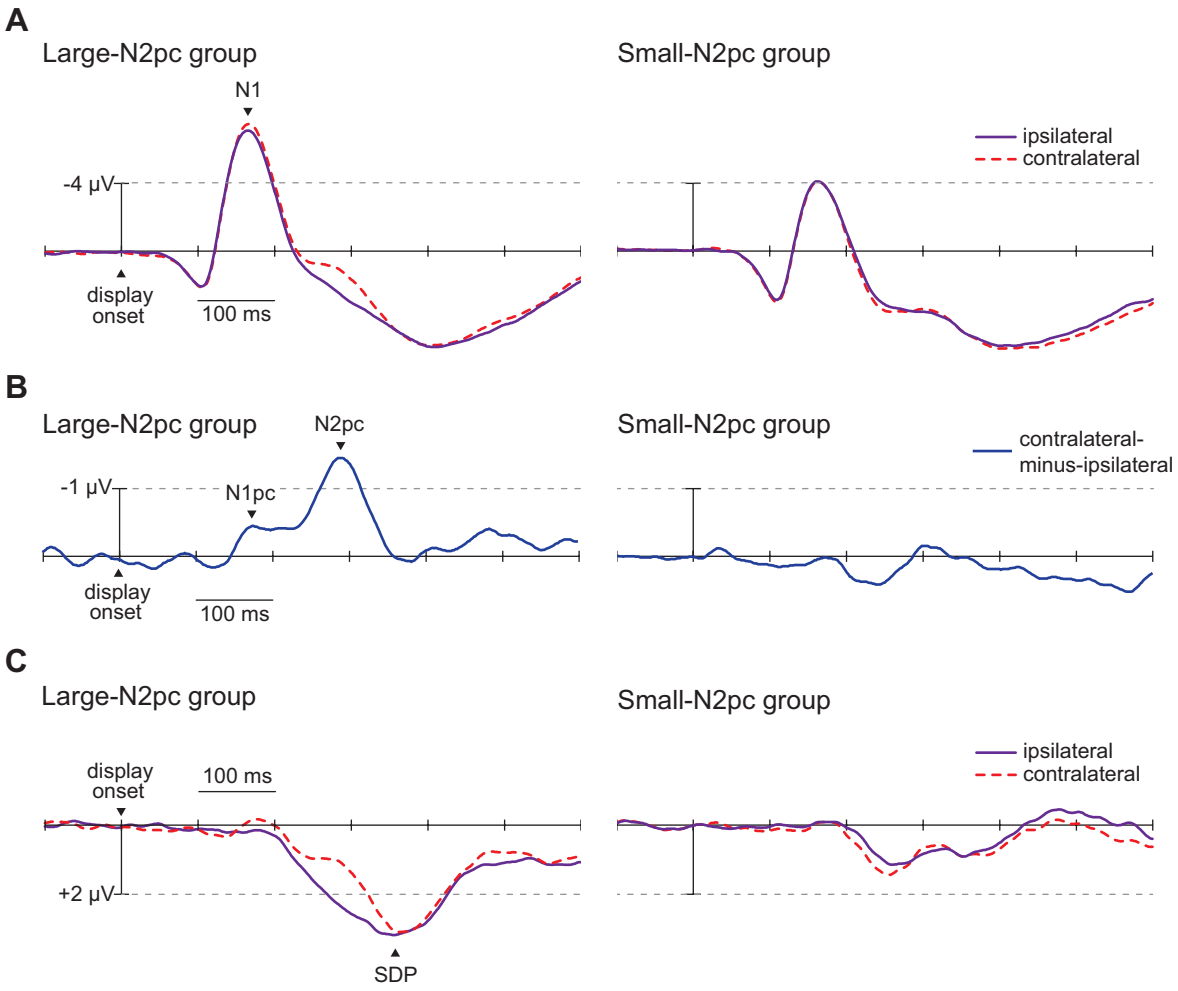

Figure 8. ERP visualizations of N2pc's relationship with N1, N1pc, and SDP. (**A**) Target-present ERPs recorded over the contralateral and ipsilateral scalp, separately for sub-groups (N=13 each) of participants with the largest N2pc and smallest N2pc. (**B**) Contralateral-minus-ipsilateral difference waves for the same N=13 sub-groups of participants. (**C**) Target-present-minus-target-absent difference waves for the same N=13 sub-groups of participants.

4. Discussion

The present work was motivated by a pair of previous studies in which the N2pc was or was not observed in a task involving the detection of an unpredictable orientation singleton (Luck & Hillyard, 1994a; Schubö et al., 2004). Luck and Hillyard did not observe a significant N2pc (with a set size 8) and concluded that it was absent because the singleton detection task

discourages participants from utilizing a distractor-filtering operation that was hypothesized to generate the N2pc. Schubö et al. replicated the null results for small set sizes (2, 4, 6) but reported an N2pc for larger set sizes (including set size 10 in their second experiment). Schubö et al. did not make any conclusions about the functional significance of the N2pc, but their observation of an N2pc in the singleton detection task using set sizes of 10 and above would seem to argue against the distractor-filtering hypothesis. Resolution of this conflicting pattern of results would have important implications for our understanding of the processes underlying the N2pc and of the nature of attention deficits that have been highlighted using the N2pc (e.g., Wang et al., 2016).

Our results show that the N2pc is, in fact, observable in the singleton detection task that was used by Luck and Hillyard (1994a) to discourage spatial filtering. The N2pc reported here was highly reliable (split-half reliability = 0.96), was predictably larger in the lower field (cf. Luck et al., 1997), was earlier on repeat-orientation trials than on change-orientation trials presumably due to inter-trial priming of pop-out (Eimer et al., 2010; although the present latency difference was only marginally significant), and was earlier for fast-response trials than for slow-response trials. Luck and Hillyard (1994a; see also Luck, 2012) interpreted their negative finding as evidence for the filtering hypothesis, and by the same rationale, the present N2pc results could be taken as evidence against the filtering hypothesis. Although it is not possible to definitively rule out filtering as contributing to the N2pc in the singleton detection paradigm (or other paradigms), it is reasonable at this point to conclude that the singleton detection paradigm yields no evidence for the filtering hypothesis.

The present results also have implications for our understanding of the hypothetical strategies that participants may use to search for visual targets. When searching for a singleton

with fixed features, participants may use a strategy that compares information from the search array to representations of the relevant stimulus feature (feature search mode) or a strategy that detects elements in the display that differ from other elements (singleton detection mode; Bacon & Egeth, 1994). Experimenters can make the singleton detection strategy more likely to be utilized by making the features of the target and distractors swap randomly across trials, as was the case in the present experiment, or make the feature search strategy more likely by presenting multiple singletons in the same display. Luck and Hillyard's (1994a, 1994b) N2pc results would seem to suggest that different selection processes are involved in singleton detection tasks (where N2pc was reported to be absent) and feature-based search tasks (where N2pc is reliably observed) or even that singleton detection is accomplished without having to attend to the spatial location of the singleton (Luck & Ford, 1998; Luck et al., 1997; Treisman & Gelade, 1980). The present results suggest otherwise. We conclude that the attentional processes that underlie the N2pc are involved in singleton detection as well as feature search and surmise that any differences between the two search modes are likely due to different control-level processes rather than the actual selection processes.

The present study did not include a feature-search condition, but based on prior studies it would be reasonable to expect the N2pc to be larger and to occur earlier if the orientations of the target and nontarget were fixed across trials. There are many possible explanations for this predicted difference (which is why the comparison was not made). Perhaps the simplest explanation is that a top-down attentional set for the target's orientation and a history of selecting the same item across all trials would combine to boost the salience of a fixed-orientation target over that of a variable-orientation target. This explanation fits well with the known effects of salience on N2pc amplitude and latency (e.g., see Figure 5 of Gaspar & McDonald, 2014). Of

course, the distractor-filtering hypothesis could be adapted to allow for some filtering to occur in singleton detection tasks even though such filtering would impair singleton detection. This new filtering view would then be able to handle the observation of an N2pc in our task as well as a magnitude difference between feature search mode and singleton detection mode. It is less clear why filtering would occur later in singleton detection tasks than in feature search tasks, however. More generally, adapting the filtering hypothesis to fit each new set of data would "run the risk of making the filtering hypothesis unfalsifiable" (Luck, 2012, p. 354).

Although the present results show definitively that the N2pc is observable in the singleton detection task, it is important to note that there was considerable variability across participants in the magnitude of the N2pc, with roughly one quarter of the participants essentially showing no N2pc (see Figures 2C and 7C). At present, the underlying causes for these individual differences are unclear. Prior research has shown that in enumeration tasks, wherein participants must indicate the number of targets in the display, the magnitude of N2pc increases as additional targets are added to the display until the number of targets reaches an individual subject's visual working memory capacity (which is 3-4 items, on average; Ester, Drew, Klee, Vogel, & Awh, 2012). Thus, it is possible that individual differences in visual working memory capacity contributed to the N2pc magnitude differences in the present study. We did not measure memory capacity in the present study, and so future studies are necessary to better understand the factors contributing to the individual differences in singleton detection.

Our more exploratory analyses revealed three potentially important findings. First, a lateralized asymmetry in the amplitude of the posterior N1 was evident, especially for lower-field targets (Figures 4B and 4D) and on fast-response trials (Figure 5B). Wascher and Beste (2010b) labelled this asymmetry the N1pc and hypothesized that it reflects an early encoding of

stimulus localization. Second, the target singleton was found to elicit a bilaterally symmetrical ERP positivity—the SDP—over the posterior scalp. Subtraction of ERPs elicited by target-absent displays helped to reveal SDP and to distinguish it from the more anterior P3b. Compared to the P3b, the SDP was seen over more posterior scalp regions, had an earlier peak (350-400 ms vs. 425-475 ms of the P3b), and was sustained for a shorter duration. Unlike the P3b, the SDP had clear maxima over both the contralateral and ipsilateral occipital hemispheres, suggesting that the component is generated bilaterally in visual regions of the posterior cortex. Most notably, the SDP began 33–34 ms prior to the onset of the N2pc and was found to be significant in a 50-ms interval that preceded N2pc onset, which indicates that the processes driving the SDP commence prior to the deployment of attention (as indexed by the N2pc). The onset latency of the SDP was also found to be predictive of manual response speed, buttressing our conclusion that the component is associated with singleton detection. Third, the magnitude of the N2pc was found to correlate with the magnitudes of the posterior N1, the N1pc, and the SDP. Specifically, participants were more likely to have a large-amplitude N2pc if at least one of these earlier components was large.

In light of the present findings, we propose the following ERP chronometry of visual singleton detection. As discussed elsewhere (e.g., Jannati, Gaspar, & McDonald, 2013; Luck & Hillyard, 1994a), the visual system encodes features contained within the display in parallel, giving rise to the earliest visual evoked potential components, including the C1 from striate cortex that peaks about 90 ms after display onset and the P1 from extrastriate cortex that peaks 10–20 ms later (e.g., Di Russo, Martinez, Sereno, Pitzalis, & Hillyard, 2002). Stimulus displays that are processed actively for a task-relevant discontinuity trigger a facilitatory process that amplifies the posterior N1 roughly 150–200 ms after display onset (Vogel & Luck, 2000).

Enhancement of visual processing is global at this stage because the observer must monitor the entire display for a target (but in other paradigms, the enhancement may be confined to attended region of the display; Mangun, 1995; Vogel & Luck, 2000; Di Russo, Martinez, & Hillyard, 2003; see also Arnott, Pratt, Shore, & Alain, 2001). The facilitatory process that is hypothesized to result in bilateral N1 enhancement may be analogous to a hypothetical "blaster" process that enables observers to pick out task-relevant visual targets that appear in a serial stream of nontarget items (Wyble, Bowman, & Nieuwenstein, 2009). At about the same time the blaster boosts processing of all display items, the visual input is parsed based on local contrast and task relevance to form a map of attentional priority (Constantinidis & Steinmetz, 2005; Fecteau & Munoz, 2006; Itti & Koch, 2000; Tan & Wyble, 2015). The locations of salient discontinuities are coarsely encoded on the attention-priority map and are more precisely pinpointed through iterative communications between neurons on the priority map and neurons in striate and extrastriate visual areas that have smaller receptive fields (Callahan-Flintoft, Chen, & Wyble, 2018; Tan & Wyble, 2015; Tsotsos et al., 1995). The visual system begins to accrue evidence for the presence of a task-relevant singleton after some initial iterative exchanges between the attention-priority map and the rest of the visual system, giving rise to a bilateral SDP over the occipital scalp. The detection of the task-relevant singleton is hypothesized to occur once the SDP reaches some critical threshold. Localization of this singleton is manifested by a contralateral negativity in the time range of the N1 (N1pc), which depends on the salience of the singleton and the degree of inter-item competition in the visual field (Verleger et al., 2012; Wascher & Beste, 2010a, 2010b). Finally, after the relevance and localization of the singleton are established and encoded, the N2pc reflects the allocation of attention to the singleton's location in order to evaluate its featural properties.

In conclusion, the N1pc and the subsequent N2pc are hypothesized to reflect transient processes associated with spatial encoding and attentional selection, respectively, while the SDP is hypothesized to reflect longer-lasting processes associated with the (possibly conscious) detection of a task-relevant singleton. The duration of the N2pc is in line with estimates of how fast attention can be deployed to different objects of potential interest (Woodman & Luck, 1999, 2003), while the duration of the SDP is more in line with estimates of how long attention dwells on individual objects of interest (i.e., attentional dwell time; Duncan, Ward, & Shapiro, 1994).

5. References

Arnott, S. R., Pratt, J., Shore, D. I., & Alain, C. (2001). Attentional set modulates visual areas: An event-related potential study of attentional capture. *Cognitive Brain Research, 12(3)*, 383-395. https://doi.org/10.1016/S0926-6410(01)00066-0

Bacon, W. F., & Egeth, H. E. (1994). Overriding stimulus-driven attentional capture. *Perception & Psychophysics*, *55(5)*, 485–496. https://doi.org/10.3758/BF03205306

Callahan-Flintoft, C., Chen, H., & Wyble, B. (2018). A hierarchical model of visual processing simulates neural mechanisms underlying reflexive attention. *Journal of Experimental Psychology: General*, *147(9)*, 1273–1294. http://doi.org/10.1037/xge0000484

Christie, G. J., Livingstone, A. C., & McDonald, J. J. (2015). Searching for inefficiency in visual search. *Journal of Cognitive Neuroscience*, *27(1)*, 46–56. https://doi.org/10.1162/jocn_a_00716

Constantinidis, C., & Steinmetz, M. A. (2005). Posterior parietal cortex automatically encodes the location of salient stimuli. *Journal of Neuroscience*, *25(1)*, 233–238. https://doi.org/10.1523/JNEUROSCI.3379-04.2005

Di Russo, F., Martínez, A., & Hillyard, S. A. (2003). Source analysis of event-related cortical activity during visuo-spatial attention. *Cerebral Cortex*, *13(5)*, 486–499. https://doi.org/10.1093/cercor/13.5.486

Di Russo, F., Martínez, A., Sereno, M. I., Pitzalis, S., & Hillyard, S. A. (2002). Cortical sources of the early components of the visual evoked potential. *Human Brain Mapping*, *15(2)*, 95–111. https://doi.org/10.1002/hbm.10010

Duncan, J., Ward, R., & Shapiro, K. (1994). Direct measurement of attentional dwell time in human vision. *Nature*, *369*, 313–315. https://doi.org/10.1038/369313a0

Eimer, M. (1996). The N2pc component as an indicator of attentional selectivity. *Electroencephalography & Clinical Neurophysiology, 99(3)*, 225–234. https://doi.org/10.1016/0013-4694(96)95711-9

Eimer, M., & Grubert, A. (2014). Spatial attention can be allocated rapidly and in parallel to new visual objects. *Current Biology*, *24(2)*, 193–198. https://doi.org/10.1016/j.cub.2013.12.001

Eimer, M., Kiss, M., & Cheung, T. (2010). Priming of pop-out modulates attentional target selection in visual search: Behavioural and electrophysiological evidence. *Vision Research*, *50(14)*, 1353–1361. https://doi.org/10.1016/j.visres.2009.11.001

Ester, E. F., Drew, T., Klee, D., Vogel, E. K., & Awh, E. (2012). Neural measures reveal a fixed item limit in subitizing. *Journal of Neuroscience*, *32(21)*, 7169–7177. https://doi.org/10.1523/JNEUROSCI.1218-12.2012

Fecteau, J. H., & Munoz, D. P. (2006). Salience, relevance, and firing: a priority map for target selection. *Trends in Cognitive Sciences*, *10(8)*, 382–390. https://doi.org/10.1016/j.tics.2006.06.011

Gaspar, J. M., Christie, G. J., Prime, D. J., Jolicœur, P. & McDonald, J. J. (2016). Inability to suppress salient distractors predicts low visual working memory capacity. *Proceedings of the National Academy of Science, U.S.A., 113(13)*, 3693–3698. https://doi.org/10.1073/pnas.1523471113

Gaspar, J. M., & McDonald, J. J. (2014). Suppression of salient objects prevents distraction in visual search. *Journal of Neuroscience*, *34(16)*, 5658–5666. https://doi.org/10.1523/JNEUROSCI.4161-13.2014

Gaspelin, N. & Luck, S. J. (2018). Combined electrophysiological and behavioral evidence for the suppression of salient distractors. *Journal of Cognitive Neuroscience*, *30(9)*, 1265–1280. https://doi.org/10.1162/jocn_a_01279

Green, J. J., Conder, J. A., & McDonald, J. J. (2008). Lateralized frontal activity elicited by attention-directing visual and auditory cues. *Psychophysiology, 45(4)*, 579-587. https://doi.org/10.1111/j.1469-8986.2008.00657.x

Hickey, C., Di Lollo, V. & McDonald, J. J. (2009). Electrophysiological indices of target and distractor processing in visual search. *Journal of Cognitive Neuroscience, 21(4)*, 760–775. https://doi.org/10.1162/jocn.2009.21039

Hickey, C., McDonald, J. J., & Theeuwes, J. (2006). Electrophysiological evidence of the capture of visual attention. *Journal of Cognitive Neuroscience, 18(4)*, 604–613. https://doi.org/10.1162/jocn.2006.18.4.604

Itti, L., & Koch, C. (2001). Computational modelling of visual attention. *Nature Reviews Neuroscience*, *2*, 194–203. https://doi.org/10.1038/35058500

Jannati, A., Gaspar, J. M., & McDonald, J. J. (2013). Tracking target and distractor processing in fixed-feature visual search: Evidence from human electrophysiology. *Journal of Experimental Psychology: Human Perception and Performance*, *39(6)*, 1713–1730. https://doi.org/10.1037/a0032251

Luck, S. J. (2012). Electrophysiological correlates of the focusing of attention within complex visual scenes: N2pc and related ERP components. In S. J. Luck & E. S. Kappenman (Eds.), *The Oxford Handbook of Event-Related Potential Components* (pp. 329–360). Oxford: Oxford University Press.

Luck, S. J. & Ford, M. A. (1998). On the role of selective attention in visual perception. *Proceedings of the National Academy of Sciences U.S.A., 95(3)*, 825–830. https://doi.org/10.1073/pnas.95.3.825

Luck, S. J., Fuller, R. L., Braun, E. L., Robinson, B., Summerfelt, A., & Gold, J. M. (2006). The speed of visual attention in schizophrenia: Electrophysiological and behavioral evidence. *Schizophrenia Research*, *85(1–3)*, 174–195. https://doi.org/10.1016/j.schres.2006.03.040

Luck, S. J., Girelli, M., McDermott, M. T. & Ford, M. A. (1997). Bridging the gap between monkey neurophysiology and human perception: An ambiguity resolution theory of visual selective attention. *Cognitive Psychology, 33(1)*, 64–87. https://doi.org/10.1006/cogp.1997.0660

Luck, S. J., & Gold, J. M. (2008). The construct of attention in schizophrenia. *Biological Psychiatry*, *64(1)*, 34–39. https://doi.org/10.1016/j.biopsych.2008.02.014

Luck, S. J., & Hillyard, S. A. (1990). Electrophysiological evidence for parallel and serial processing during visual search. *Perception & Psychophysics*, *48(6)*, 603–617. https://doi.org/10.3758/BF03211606

Luck, S. J. & Hillyard, S. A. (1994a). Spatial filtering during visual search: evidence from human electrophysiology. *Journal of Experimental Psychology: Human Perception and Performance, 20(5)*, 1000–1014. https://doi.org/10.1037/0096-1523.20.5.1000

Luck, S. J., & Hillyard, S. A. (1994b). Electrophysiological correlates of feature analysis during visual search. *Psychophysiology, 31(3)*, 291–308. https://doi.org/10.1111/j.1469-8986.1994.tb02218.x

Maljkovic, V., & Nakayama, K. (1994). Priming of pop-out: I. Role of features. *Memory & Cognition*, *22(6)*, 657–672. https://doi.org/10.3758/BF03209251

Mangun, G. R. (1995). Neural mechanisms of visual selective attention. *Psychophysiology*, *32(1)*, 4–18. https://doi.org/10.1111/j.1469-8986.1995.tb03400.x

Mazza, V., Turatto, M., & Caramazza, A. (2009). Attention selection, distractor suppression and N2pc. *Cortex*, *45(7)*, 879–890. https://doi.org/10.1016/j.cortex.2008.10.009

McDonald, J. J., Green, J. J., Jannati, A., & Di Lollo, V. (2013). On the electrophysiological evidence for the capture of visual attention. *Journal of Experimental Psychology: Human Perception and Performance*, *39(3)*, 849–860. https://doi.org/10.1037/a0030510

Meinecke, C., & Donk, M. (2002). Detection performance in pop-out tasks: Nonmonotonic changes with display size and eccentricity. *Perception*, *31(5)*, 591–602. https://doi.org/10.1068/p3201

Miller, J., Patterson, T., & Ulrich, R. (1998). Jackknife-based method for measuring LRP onset latency differences. *Psychophysiology*, *35(1)*, 99–115. https://doi.org/10.1111/1469-8986.3510099

Phipson, B., & Smyth, G. K. (2010). Permutation P-values should never be zero: calculating exact P-values when permutations are randomly drawn. *Statistical Applications in Genetics and Molecular Biology*, *9(1)*, Article 39. https://doi.org/10.2202/1544-6115.1585

Schubö, A., Schröger, E., & Meinecke, C. (2004). Texture segmentation and visual search for pop-out targets: An ERP study. *Cognitive Brain Research*, *21(3)*, 317–334. https://doi.org/10.1016/j.cogbrainres.2004.06.007

Tan, M., & Wyble, B. (2015). Understanding how visual attention locks on to a location: Toward a computational model of the N2pc component. *Psychophysiology*, *52(2)*, 199–213. https://doi.org/10.1111/psyp.12324

Theeuwes, J. (2010). Top–down and bottom–up control of visual selection. *Acta Psychologica*, *135(2)*, 77–99. https://doi.org/10.1016/j.actpsy.2010.02.006

Treisman, A. M., & Gelade, G. (1980). A feature-integration theory of attention. *Cognitive Psychology*, *12(1)*, 97–136. https://doi.org/10.1016/0010-0285(80)90005-5

Tsotsos, J. K., Culhane, S. M., Wai, W. Y. K., Lai, Y., Davis, N., & Nuflo, F. (1995). Modeling visual attention via selective tuning. *Artificial intelligence*, *78(1-2)*, 507–545. https://doi.org/10.1016/0004-3702(95)00025-9

Verleger, R., vel Grajewska, B. Ż., & Jaśkowski, P. (2012). Time-course of hemispheric preference for processing contralateral relevant shapes: P1pc, N1pc, N2pc, N3pc. *Advances in cognitive psychology*, *8(1)*, 19–28. https://doi.org/10.2478/v10053-008-0098-9

Vogel, E. K., & Luck, S. J. (2000). The visual N1 component as an index of a discrimination process. *Psychophysiology*, *37(2)*, 190–203. https://doi.org/10.1111/1469-8986.3720190

Wang E, Sun L, Sun M, Huang J, Tao Y et al. (2016). Attentional selection and suppression in children with attention-deficit/hyperactivity disorder. *Biological Psychiatry: CNNI, 1(4)*, 372–380. https://doi.org/10.1016/j.bpsc.2016.01.004

Wascher, E. & Beste, C. (2010a). Spatial representations as an emergent feature of perceptual processing. *Journal of Psychophysiology, 24(3)*, 161-172. https://doi.org/10.1027/0269-8803/a000007

Wascher, E. & Beste, C. (2010b). Tuning perceptual competition. *Journal of Neurophysiology, 103(2)*, 1057-1065. https://doi.org/10.1152/jn.00376.2009

Woodman, G. F. & Luck, S. J. (1999). Electrophysiological measurement of rapid shifts of attention during visual search. *Nature, 400*, 867–869. https://doi.org/10.1038/23698

Woodman, G. F., & Luck, S. J. (2003). Serial deployment of attention during visual search. *Journal of Experimental Psychology: Human Perception and Performance*, *29(1)*, 121–138. https://doi.org/10.1037/0096-1523.29.1.121

Wyble, B., Bowman, H., & Nieuwenstein, M. (2009). The attentional blink provides episodic distinctiveness: Sparing at a cost. *Journal of Experimental Psychology: Human Perception and Performance, 35(3)*, 787-807. https://doi.org/10.1037%2Fa0013902